Phase transition of MnF_2 driven by shock compression at pressure of up to 33 GPa

Teruhisa Hongo,[1,*] Kazutaka G. Nakamura,[1,†,‡] Toshiyuki Atou,[1,†,§] Masae Kikuchi,[3] Kunio Yubuta,[2] Shun Itoh,[2] Keiji Kusaba,[2] Kiyoto Fukuoka,[2] and Ken-ichi Kondo[1]

[1]*Materials and Structures Laboratory, Tokyo Institute of Technology R3-10, 4259 Nagatsuta, Yokohama 226-8503, Japan*

[2]*Institute for Materials Research, Tohoku University, 2-1-1 Katahira, Aoba, Sendai 980-8577, Japan*

[3]*Kansei-Fukushi Research Center, Tohoku Fukushi University, Kunimigaoka 6-149-1, Aoba-ku, Sendai 989-3201, Japan*

(Received 21 March 2007; published 28 September 2007)

Rutile-type MnF_2 was shock loaded at pressures of 3.6–33.4 GPa by the impact of flyer plates accelerated by a propellant gun. Recovered samples were examined by x-ray powder diffraction analysis and transmission electron microscopy (TEM). A phase transition from the rutile-type structure to the α-PbO_2-type structure was found above 3.6 GPa. The yield of the α-PbO_2 phase in the recovered samples increased for pressures of up to about 10 GPa and decreased at higher pressures. This phenomenon can be explained by a residual temperature effect. A lamellar pattern consisting of two crystalline phases (rutile and α-PbO_2-type MnF_2) was observed in the shocked sample by TEM observation. The shock-induced phase transition from the rutile-type structure to the α-PbO_2-type structure was inferred to proceed via fluorite-related structures or a $PbCl_2$-type structure by comparison with results of previous static high-pressure experiments.

DOI: 10.1103/PhysRevB.76.104114 PACS number(s): 62.50.+p, 61.50.Ks, 64.60.−i, 91.60.Gf

I. INTRODUCTION

The high-pressure polymorphism in AX_2 compounds has attracted considerable attention among geophysicists and has been intensively studied in connection with the phase stability of SiO_2 in the earth.[1–5] A lot of polymorphisms in AX_2 compounds have been discovered owing to the marked progress in experimental techniques.[1] Under high pressure, many structural phase transitions occur with increasing cation coordination number (CN). The CN in AX_2 compounds now ranges from 4 in the quartz structure to 11 in the Ni_2In structure.[6] Four-coordinated AX_2 compounds were thought to transform into the six-coordinated rutile-type structure, and then into the eight-coordinated fluorite-related structure.[7] However, rutile-type TiO_2 transforms into the baddeleyite-type structure (CN=7),[8] whereas the other rutile-type AX_2 compounds (such as SiO_2, RuO_2, and SnO_2) transform into a modified fluorite structure ($Pa\bar{3}$-type, CN=6+2).[1–3]

MnF_2 is stable as the rutile-type structure at ambient pressure and temperature, although the Mn^{2+} cation radius is fairly large as a six-coordinated cation in the rutile structure.[9] High-pressure phase transitions in MnF_2 have already been studied by both static and dynamic high-pressure compression.[9–16] German and Podurets reported shock Hugoniot measurement and shock recovery experiments on MnF_2.[10] In the Hugoniot measurement, they found two kinks at 4 and 13 GPa and attributed them as phase transitions to the α-PbO_2-type structure and into the $PbCl_2$-type structure, respectively. In the static high-pressure experiments, rutile-type MnF_2 transforms into the fluorite (cubic) structure or a distorted fluorite structure above 3.3 GPa and into the $PbCl_2$-type structure at 15 GPa.[12,13] Shinoda *et al.*[14] and Hamaya and Hara[15] revealed that the cubic phase had the $Pa\bar{3}$-type structure, whereas the distorted fluorite phase was related to the orthorhombic ZrO_2-type structure. The pressure-temperature phase diagram of MnF_2 determined by static experiments contains no definite stable region for the α-PbO_2 phase.[12] Therefore, the α-PbO_2 phase formation mechanism driven by shock waves has not been clarified completely and little is known about the dynamic response of rutile-type MnF_2.

The aim of the present work is to investigate the phase transition mechanism of MnF_2 driven by shock waves. In this study, we performed a shock recovery experiment on MnF_2 at pressures of up to 33.4 GPa and examined the recovered samples by x-ray diffraction analysis and transmission electron microscopy (TEM). Our final goal is to discuss the phase transition mechanism and crystallographic relationship between the low-pressure and high-pressure phases.

II. EXPERIMENTAL PROCEDURE

The sample used was MnF_2 powder with a purity of 99.9% obtained from Rare Metallic Co., Ltd. The powdered sample was hot pressed in graphite dies at a temperature of 680 °C for 1 h at 30 MPa under flowing argon. The sintered sample was formed into a disk of 14 mm diameter and 1 mm thickness. By x-ray powder diffraction analysis, this sintered sample was confirmed to have the rutile-type structure. Bulk density of the sintered sample was determined by the Archimedean method and found to be 98% of the crystal density (3890 kg/m^3). On the other hand, high-crystallinity samples were also prepared by melting the sintered samples for the TEM observation. The crystallite sizes were larger than ~100 μm.

A series of shock recovery experiments was carried out using a 20 mm bore propellant gun with impact velocities of up to 1.6 km/s. Figure 1 shows a schematic of the shock recovery experiment using the propellant gun. The sample disk was encased in an iron container for the purpose of protection from destructive shock. The sample container was impacted by a flyer plate. Four materials (copper, Al2024, Teflon, or high-density polyethylene (HDPE)) with different impedances were used for the flyer plate. We controlled shock pressure by changing impact velocity and the flyer plate materials. Thickness of the flyer plate was 5 mm for

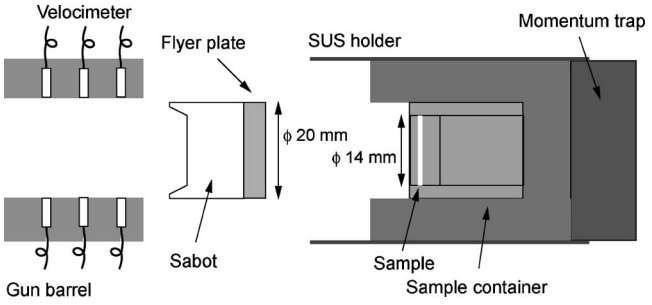

FIG. 1. Schematic of the shock recovery experiment using a propellant gun. The velocity meter composed of the three lasers with photodiode detectors was used to measure the projectile velocity.

copper, Al2024, and Teflon and was 10 mm for HDPE. The shock duration is estimated to be approximately 1.6 μs when the Al2024 flyer impacted with flyer velocity of 1.4 km/s. Impact velocity was measured using a velocimeter consisting of three lasers with photodiode detectors. The pressure in the container was estimated using the measured impact velocity of the flyer and the impedance matching method.[17] The shocked state in the sample was considered to be equilibrated with that in the container via multiple shock reverberation across the sample-container boundaries, and the final pressure realized in the sample would be almost the same as the pressure achieved in the container. Shock-recovered samples were examined by x-ray powder diffraction analysis using a diffractometer with monochromatic Cu $K\alpha$ radiation. TEM observation was conducted with a JEM-2000EX II transmission electron microscope operated at 200 kV for low-magnification TEM observation and with a JEM-2010 operated at 200 kV for high-resolution transmission electron microscopy (HRTEM) observation. The recovered sample was crushed, and an edge of a fragment was examined by TEM and HRTEM observations.

III. RESULTS

Figure 2(a) shows the x-ray diffraction pattern from a pristine sample of MnF_2. The diffraction peaks at $2\theta = 25.8°$ and 32.7° are assigned to the 110 and 101 reflections from rutile-type MnF_2, respectively. Figures 2(b)–2(f) show the x-ray diffraction patterns from shock-recovered MnF_2 at pressures between 3.6 and 33.4 GPa. The X GPa sample denotes, hereafter, the sample recovered at the maximum pressure of X GPa, for example, the 3.6 GPa sample. New diffraction peaks other than those of the rutile phase were observed in the 3.6 GPa sample at 23.6° and 28.9°, which are assigned to the 110 and 111 reflections of α-PbO_2-type MnF_2 with the space group $Pbcm$, respectively. The linewidths of these new peaks are broader than those of rutile-type MnF_2. The intensities of these new peaks increased in the recovered samples for high pressures of up to 11.8 GPa and decreased in the 11.8 and 33.4 GPa samples. On the other hand, the peak intensities of rutile-type MnF_2 decreased in the recovered samples for high pressures of up to 11.8 GPa and increased in the 11.8 and 33.4 GPa samples.

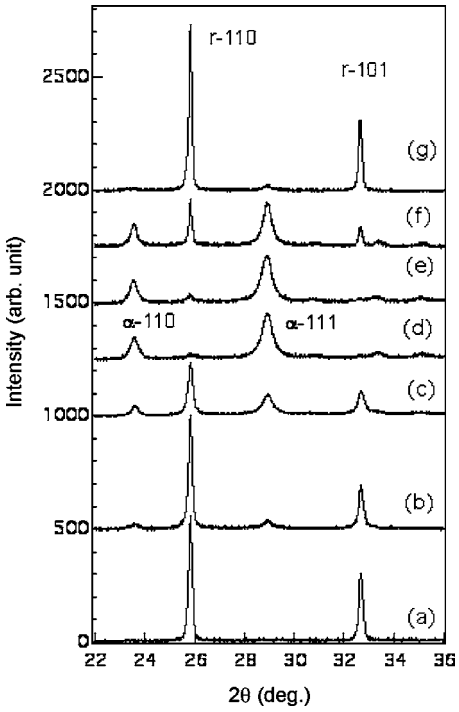

FIG. 2. X-ray diffraction patterns of unshocked and shocked samples. (a) Starting material (rutile structure). [(b)–(g)] Shock-recovered sample for 3.6, 6.5, 8.3, 11.8, 18.2, and 33.4 GPa. Each shock-recovered sample exhibited a mixed phase of rutile-type and α-PbO_2-type MnF_2. Each x-ray diffraction pattern is normalized by $I_\alpha + I_r$, where I_α and I_r represent the x-ray integrated intensities of α-PbO_2-type MnF_2 (111 peak) and rutile-type MnF_2 (110 peak), respectively.

We estimate the apparent yield (Y) of α-PbO_2-type MnF_2 using

$$Y = I_\alpha/(I_\alpha + I_r),$$

where I_α and I_r represent the x-ray diffraction integrated intensities of α-PbO_2-type MnF_2 (111 peak) and rutile-type MnF_2 (110 peak), respectively.[18] Figure 3 shows the yield of α-PbO_2-type MnF_2 plotted as a function of shock pressure. α-PbO_2-type MnF_2 appeared above ~3 GPa. The amount of the α-PbO_2-type phase increased with increasing pressure up to about 10 GPa and then decreased with increasing pressure up to 33.4 GPa.

Figure 4(a) shows a low-magnification TEM image of the 9 GPa sample. Corresponding diffraction patterns are shown in Fig. 4(b). Lamellar textures were frequently observed in the recovered sample. The electron diffraction pattern of this lamellar texture can be interpreted as the superposition of rutile-type and α-PbO_2-type MnF_2 patterns. The crystallographic relationship between both phases can be expressed as $(10\bar{1})_r \| (001)_\alpha$ and $[111]_r \| [110]_\alpha$, where r and α represent the rutile-type and α-PbO_2-type structures, respectively. Same relationship is also observed in TEM image of the 4.4 GPa sample.[19]

Figure 5(a) shows an HRTEM image of the 9 GPa sample, which confirms the constitution and fine structure of

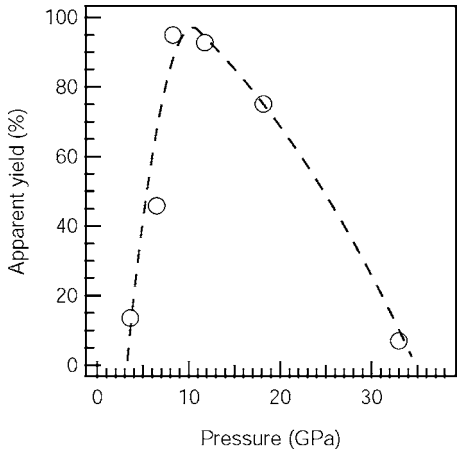

FIG. 3. Apparent yield of α-PbO_2-type MnF_2 plotted as a function of pressure. Open circles represent the yield of the α-PbO_2-type phase at each shock pressure. The dashed line is a guide for the eyes.

these lamellae. The boundaries between rutile-type and α-PbO_2-type MnF_2 are indicated by triangles. The electron diffraction pattern [inset of Fig. 5(a)] can be interpreted as the superposition of the rutile and α-PbO_2 patterns with the same crystallographic relationship as that in Fig. 4(b). Fast Fourier transforms (FFTs) were taken from within the crystalline matrix of areas b and c in Fig. 5(a), and the FFT patterns are shown in Figs. 5(b) and 5(c). The FFT patterns taken from area b [Fig. 5] showed a reciprocal lattice indicative of the rutile-type structure ([111] zone axis). On the

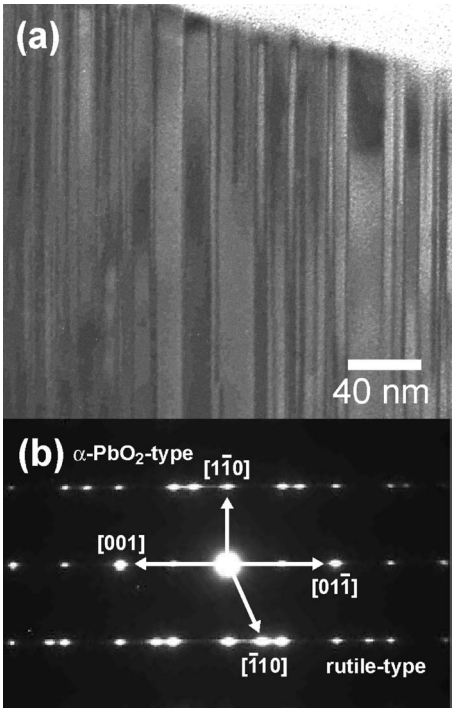

FIG. 4. (a) Typical low-magnification TEM image and (b) the corresponding diffraction pattern of shock-recovered sample at pressure of 9.0 GPa.

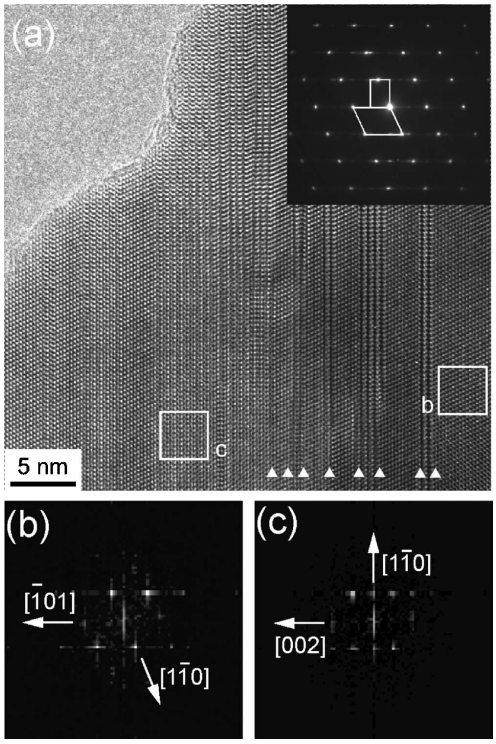

FIG. 5. High-resolution TEM image of the shock-recovered sample for 9.0 GPa. (a) Bright-field image showing that the lamella structure consisted of the rutile-type and α-PbO_2-type phases. The boundaries of these phases are indicated by triangles. The inset shows the corresponding diffraction pattern. Fast Fourier transforms (FFTs) were taken from within areas b and c in (a); the FFT patterns are shown in (b) and (c).

other hand, the FFT patterns from area c [Fig. 5(c)] showed a reciprocal lattice indicative of the α-PbO_2-type structure ([110] zone axis). These α-PbO_2-type phases nucleated throughout the rutile slabs and formed a thin lamellar pattern with a spacing of less than 10 nm. In shock-loaded quartz or feldspars, lamellar patterns were sometimes observed, in which the lamellae consist of crystalline and amorphous phases.[20–22] In the present study, the lamellar pattern consisted of two crystalline phases (rutile-type and α-PbO_2-type MnF_2). This kind of lamella pattern is seldom observed in high-pressure phase transitions,[18,23] as far as we know. Such features of the texture indicate that the observed rutile-type–α-PbO_2-type phase transition has a displacive phase transition mechanism and no atomic diffusion is required.

IV. DISCUSSION

In this study, the shock-induced rutile-type to α-PbO_2-type phase transition of MnF_2 was observed above 3.6 GPa in the shock recovery experiments. Although the volume of α-PbO_2-type MnF_2 is smaller by 1.8% than that of rutile-type MnF_2, α-PbO_2-type MnF_2 is a metastable phase under ambient temperature and pressure, rather than a quenched high-pressure phase, because no stable region for the α-PbO_2 phase has been reported so far in the P-T dia-

gram of MnF_2.[12] Therefore, the direct transformation from the rutile-type structure to the α-PbO_2-type structure is unlikely to occur. Also, the transformation of the rutile-type–α-PbO_2-type structure is thought of as a reconstructive type of transformation from the point of view of crystal chemistry[18,24] so that this direct transformation is unfavorable during the short duration time (~ 1 μs) in the shock compression. If the rutile-type structure was assumed to transform directly to the α-PbO_2-type structure under shock compression, the cations must move considerably in the hcp framework of F^-, because the positions of Mn^{2+} are very different in these two polymorphs. Relating the potential barrier for the transition to structural change, Buerger has classified this structural transformation into the deformational type.[25] It was also experimentally shown that the heat treatment for 4 h at 400 °C under ambient pressure was necessary for the conversion of α-PbO_2-type MnF_2 to the rutile-type phase.[13]

Considering the above-mentioned and previous reports on the static high-pressure experiments,[12] rutile-type MnF_2 is considered to directly transform into the fluorite-related-type structure above ~ 3 GPa under shock compression; then, the fluorite-related-type phase transforms to the α-PbO_2-type phase during the pressure release process, resulting in the recovery of the α-PbO_2-type phase under ambient conditions. MnF_2 has two fluorite-related high-pressure phases: i.e., the $Pa\bar{3}$-type and orthorhombic phases.[12–15] It is difficult to determine which phase is realized during shock compression because shock temperature is hardly estimated accurately. Since the $Pa\bar{3}$-type phase is a high-temperature phase, the $Pa\bar{3}$-type phase might be favorable if temperature increase induced by adiabatic shock compression is taken into consideration.[12,14] There has been considerable interest in the mechanisms of phase transitions between the rutile structure and various proposed high-pressure structures. Hyde *et al.* suggested a sequential transition of the rutile–fluorite-related–α-PbO_2-type structures with only small directional displacements of atoms.[26] Such a phase transition route has been experimentally revealed in TiO_2. Note that a similar lamellar texture consisting of the rutile and α-PbO_2 phases was observed in the shock-loaded TiO_2 sample.[18] The crystallographic relationship in the TiO_2 lamellae is identical to that obtained in this study, strongly suggesting that the rutile–fluorite-related–α-PbO_2-type phase transitions also occurred in MnF_2.

To relate these crystal structures comprehensively, these structures are illustrated in Fig. 6. The $Pa\bar{3}$-type structure is illustrated as an example of the fluorite-related-type structures. Figures 6(a)–6(c) show the rutile, fluorite-related, and α-PbO_2-type structures viewed along the [100] direction, respectively. The $\{01\bar{1}\}$ plane of the rutile-type structure is parallel to the {001} plane of the fluorite-related-type and α-PbO_2-type structures. For these three structures, the sequence of stacking layers A, α, B, and β completes one unit cell [Figs. 3 (a′)–(c′)]. Layers A and B contain only Mn^{2+} cations; layers α and β contain only F^- anions. Figures 6(a) and 6(b) show the stage in a continuous topological change from a {100} plane of the rutile-type structure to a {100}

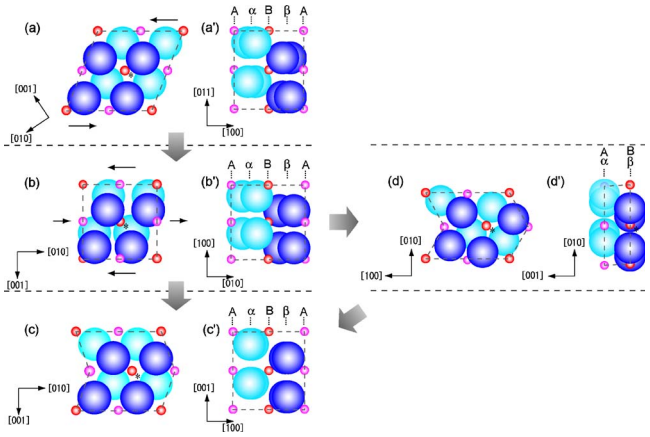

FIG. 6. (Color online) Shear mechanism from the rutile-type structure to the α-PbO_2-type structure through the fluorite-related-type ($Pa\bar{3}$-type) or $PbCl_2$-type structure. A continuous transformation can be seen from an idealized rutile-type structure in (a) to an idealized fluorite-related-type structure in (b) or an idealized $PbCl_2$-type structure in (d), and subsequently to an idealized α-PbO_2 structure in (c). Large circles, F^-; small circles, Mn^{2+}. Mn^{2+} ions are at $z=0$ and $z=1/2$, and F^- ions are at $z=1/4$ and $z=3/4$ for the rutile-type, fluorite-related-type ($Pa\bar{3}$-type), and α-PbO_2-type structures, whereas Mn^{2+} and F^- are in the same plane at $z=0$ and $z=1/2$ for the $PbCl_2$-type structure [see (a′)–(d′) and text]. (a) Rutile structure projected along the [100] direction. (a′) Rutile structure projected along the $[01\bar{1}]$ direction. (b) Fluorite-related-type ($Pa\bar{3}$-type) structure projected along the [100] direction. (b′) Fluorite-related-type ($Pa\bar{3}$-type) structure projected along the [001] direction. (c) α-PbO_2 structure projected along the [100] direction. (c′) α-PbO_2 structure projected along the [010] direction. (d) $PbCl_2$-type structure projected along the [001] direction. (d′) $PbCl_2$-type structure projected along the [100] direction.

plane of the fluorite-related-type structure. At the shock loading state, the rutile-type structure transforms into a new arrangement, shown in Fig. 6(b) with the fluorite-related-type structure by a shear mechanism moving along the arrows in Fig. 6(a). It can be readily seen that in the rutile-type structure, a shear of the $\{01-1\}$ plane will lead to a structure of the fluorite-related type. In this process, two additional long bonds are formed for the manganese-centered polyhedra. There is thus an increase in CN from 6 in the rutile-type structure, which consists of MnF_6 octahedra, to 6+2 in the fluorite-related-type ($Pa\bar{3}$) structure, which consists of MnF_8 rhombohedra. The anions in the $Pa\bar{3}$-type structure lie on 8*c* sites (u,u,u) with u being typically close to 0.345, whereas in the fluorite structure u is 0.25.[27] This difference in anion position results in the coordination polyhedron being a rhombohedron as in the $Pa\bar{3}$-type structure rather than a cube as in the fluorite-type structure. The rutile-type–fluorite-related-type transition can therefore be understood as a diffusionless process. The fluorite-related-type–α-PbO_2-type transition is considered to occur readily upon decompression, indicating that there could be a short transition pathway between these two structures. Figures 6(b) and 6(c) show a different reverse transition: gliding along arrows in Fig. 6(b), the fluorite-

related-type structure changes to the α-PbO_2-type structure. Since this movement causes the other two Mn-F bonds to lengthen in the fluorite-related-type structure, an α-PbO_2-type structure with a cation CN of 6 is produced from the fluorite-related-type ($Pa\bar{3}$) structure with a CN of 6+2. Therefore, the fluorite-related-type–α-PbO_2-type transition can also be understood as a diffusionless process.

In the static high-pressure experiments, it is reported that the $PbCl_2$-type structure is stabilized above 15 GPa. German and Podurets reported that a phase transition to the $PbCl_2$-type structure took place above ~13 GPa from shock Hugoniot measurements.[10] In the $PbCl_2$-type structure, each cation is surrounded by nine anions, six of which are at the apices of the trigonal prism with the remaining three lying beyond the centers of the three prism faces in the same plane as the cations. This structure also has close relationships between the rutile-type and α-PbO_2-type structures, as shown in Fig. 6(d). Shear movement of ions readily transforms the rutile-type structure to the $PbCl_2$-type structure and the $PbCl_2$-type structure to the α-PbO_2-type structure, as indicated by arrows. We consider that the transformation can be accomplished by such a mechanism of the rutile-type–(fluorite-related-type or $PbCl_2$-type)–α-PbO_2-type transitions within the shock process.

The amount of the α-PbO_2-type phase increased with increasing pressure up to about 10 GPa but decreased with increasing pressure up to 33.4 GPa. This phenomenon can be explained by the residual temperature effect. Shock-induced residual temperature increases with increasing pressure, resulting in a reverse conversion of the metastable α-PbO_2 phase to the stable rutile-type phase under ambient pressure. High temperature stability in α-PbO_2-type MnF_2 was reported by Lityagina *et al.*[13] At ambient pressure, the α-PbO_2-type phase transformed into the rutile-type phase after annealing at 400 °C for 4 h, while it did not change but remained as a metastable state after annealing at 300 °C for 4 h.

Interestingly, the yield of the α-PbO_2-type phase was abnormally large ($Y=50\%$) at the interface between the sample and the iron container for the sample shock loaded to 33.4 GPa, in which the average yield was only 6%, as shown in Fig. 3. The temperature history (cooling rate) of the sample at the interface differs from that inside the sample. The low-compressibility material (iron container) works as a heat sink and the sample at the interface is cooled rapidly by heat conduction. In this experiment, the interface between the sample and the container is cooled more rapidly than the inside of the sample. This observation lends support to the hypothesis that the high-pressure phase reverted to the α-PbO_2-type phase, not to the rutile-type phase, during the pressure release process, although the route for either the rutile or α-PbO_2-type structure is possible. In the static high-pressure experiments, the shear stresses promote the appearance of the α-PbO_2-type phase during the pressure release process.[13] Shock compression introduces many dislocations and defects that produce strain in the sample. Such a strained domain in the fluorite-related-type or $PbCl_2$-type phase might tend to transform into the α-PbO_2-type phase.

V. SUMMARY

The shock-induced phase transition of MnF_2 with the rutile structure was investigated at pressures of up to 33.4 GPa by conducting shock recovery experiments. α-PbO_2-type MnF_2 was observed in the recovered sample together with the rutile phase. A lamella pattern consisting of two crystal phases (rutile and α-PbO_2-type MnF_2) was observed by TEM. Rutile-type MnF_2 is considered to directly transform into high-pressure phases (fluorite-related type or $PbCl_2$ type) under the shock loading state and then into the α-PbO_2 phase under the shock unloading state. The yield of the α-PbO_2 phase was observed to be decreasing above 10 GPa. This is explained by the residual temperature effect.

ACKNOWLEDGMENTS

The authors are grateful to M. Hasegawa for constructing the experimental setup. This work was supported by a Grant-in-Aid for Science Research (A) No. 15204041 and the Collaborative Research Project of Materials and Structures Laboratory, Tokyo Institute of Technology. A part of this work was carried out under the Visiting Researcher's Program of the Laboratory for Advanced Materials, Institute for Materials Research, Tohoku University.

*Present address: Department of Resources and Environmental Engineering, School of Science and Engineering, Waseda University, 3-4-1 Okubo, Shinjuku, Tokyo 169-8555, Japan.
†Corresponding authors.
‡nakamura.k.ai@m.titech.ac.jp
§atou@msl.titech.ac.jp

[1] J. M. Leger and J. Haines, Eur. J. Solid State Inorg. Chem. **34**, 785 (1997).
[2] V. P. Prakapenka, G. Shen, L. S. Dubrovinsky, M. L. Rivers, and S. R. Sutton, J. Phys. Chem. Solids **65**, 1537 (2004).
[3] L. S. Dubrovinsky, N. A. Dubrovinskaia, V. Prakapenka, F. Seifert, F. Langenhorst, V. Dmitriev, H. P. Weber, and T. L. Bihan, Phys. Earth Planet. Inter. **143-144**, 231 (2004).
[4] A. R. Oganov, M. J. Gillan, and G. D. Price, Phys. Rev. B **71**, 064104 (2005).
[5] V. B. Prakapenka, L. S. Dubrovinsky, G. Shen, M. L. Rivers, S. R. Sutton, V. Dmitriev, H. P. Weber, and T. L. Bihan, Phys. Rev. B **67**, 132101 (2003).
[6] J. M. Leger, J. Phys. Chem. Solids **59**, 1199 (1998).
[7] Y. Syono and S. Akimoto, Mater. Res. Bull. **3**, 153 (1968).
[8] H. Sato, S. Endo, M. Sugiyama, T. Kikegawa, O. Shimomura, and K. Kusaba, Science **251**, 786 (1991).
[9] L. M. Azzaria and F. Dachille, J. Phys. Chem. **65**, 889 (1961).
[10] V. N. German and A. M. Podurets, Izv., Acad. Sci., USSR, Phys. Solid Earth **18**, 587 (1982).
[11] D. P. Dandekar and J. C. Jamieson, Trans. Am. Crystallogr. As-

soc. **5**, 19 (1969).
[12] S. S. Kabalkina, L. F. Vershchagin, and L. M. Lityagina, Sov. Phys. JETP **29**, 803 (1969).
[13] L. M. Lityagina, S. S. Kabalkina, and L. F. Vereshchagin, Sov. Phys. JETP **35**, 353 (1972).
[14] K. Shinoda, N. Hamaya, A. Kawamoto, K. Fujii, O. Shimomura, and T. Kikegawa, Rev. High Pressure Sci. Technol. **3**, 39 (1994).
[15] N. Hamaya and H. Hata, Rev. High Pressure Sci. Technol. **5**, 259 (1994).
[16] L. C. Ming, M. H. Manghnani, T. Matsui, and J. C. Jamieson, Phys. Earth Planet. Inter. **23**, 276 (1980).
[17] *High-Pressure Shock Compression of Solids*, edited by J. R. Asay and M. Shahinpoor (Springer, New York, 1992).
[18] K. Kusaba, M. Kikuchi, K. Fukuoka, and Y. Syono, Phys. Chem. Miner. **15**, 238 (1988).
[19] K. Yubuta, T. Hongo, T. Atou, K. G. Nakamura, K. Kondo, and M. Kikuchi, Solid State Commun. **143**, 127 (2007).
[20] K. J. Kingma, C. Meade, R. J. Hemley, H. Mal, and D. R. Veblen, Science **259**, 666 (1993).
[21] F. Langenhorst and A. Deutsch, Earth Planet. Sci. Lett. **125**, 407 (1994).
[22] O. Goltrant, H. Leroux, J. Doukhan, and P. Cordier, Phys. Earth Planet. Inter. **74**, 219 (1992).
[23] Y. Wang, I. Martinez, F. Guyot, and R. C. Liebermann, Science **275**, 510 (1997).
[24] M. O'Keeffe, Mater. Res. Bull. **19**, 1433 (1992).
[25] M. J. Buerger, *Phase Transformations in Solids* (Wiley, New York, 1951), pp. 183–211.
[26] B. G. Hyde, L. A. Bursill, M. O'Keeffe, and S. Andersson, Nature (London) **237**, 35 (1972).
[27] J. Haines, J. M. Leger, and O. Schulte, Science **271**, 629 (1996).